UC Irvine
Faculty Publications

Title
Evapotranspiration along an elevation gradient in California's Sierra Nevada

Permalink
https://escholarship.org/uc/item/8hj0w17b

Journal
Journal of Geophysical Research, 117(G3)

ISSN
0148-0227

Authors
Goulden, M. L.
Anderson, R. G.
Bales, R. C.
et al.

Publication Date
2012-09-01

DOI
10.1029/2012JG002027

Supplemental Material
https://escholarship.org/uc/item/8hj0w17b#supplemental

Copyright Information
This work is made available under the terms of a Creative Commons Attribution License, availalbe at https://creativecommons.org/licenses/by/3.0/

Peer reviewed

eScholarship.org Powered by the California Digital Library
University of California

Evapotranspiration along an elevation gradient in California's Sierra Nevada

M. L. Goulden,[1] R. G. Anderson,[1,2] R. C. Bales,[3,4] A. E. Kelly,[1] M. Meadows,[4] and G. C. Winston[1]

Received 13 March 2012; revised 5 July 2012; accepted 14 July 2012; published 6 September 2012.

[1] We combined observations from four eddy covariance towers with remote sensing to better understand the altitudinal patterns of climate, plant phenology, Gross Ecosystem CO_2 Uptake, and Evapotranspiration (ET) around the Upper Kings River basin in the southern Sierra Nevada Mountains. Precipitation (P) increased with elevation to ~500 m, and more gradually at higher elevations, while vegetation graded from savanna at 405 m to evergreen oak and pine forest to mid-montane forest to subalpine forest at 2700 m. CO_2 uptake and transpiration at 405 m peaked in spring (March to May) and declined in summer; gas exchange at 1160 and 2015 m continued year-round; gas exchange at 2700 m peaked in summer and ceased in winter. A phenological threshold occurred between 2015 and 2700 m, associated with the development of winter dormancy. Annual ET and Gross Primary Production were greatest at 1160 and 2015 m and reduced at 405 m coincident with less P, and at 2700 m coincident with colder temperatures. The large decline in ET above 2015 m raises the possibility that an upslope redistribution of vegetation with climate change could cause a large increase in upper elevation ET. We extrapolated ET to the entire basin using remote sensing. The 2003–11 P for the entire Upper Kings River basin was 984 mm y^{-1} and the ET was 429 mm y^{-1}, yielding a P-ET of 554 mm y^{-1}, which agrees well with the observed Kings River flow of 563 mm y^{-1}. ET averaged across the entire basin was nearly constant from year to year.

Citation: Goulden, M. L., R. G. Anderson, R. C. Bales, A. E. Kelly, M. Meadows, and G. C. Winston (2012), Evapotranspiration along an elevation gradient in California's Sierra Nevada, *J. Geophys. Res.*, *117*, G03028, doi:10.1029/2012JG002027.

1. Introduction

[2] The altitudinal patterns of plant seasonality and Evapotranspiration (ET) in the western United States are poorly characterized despite obvious practical importance. Climate and vegetation vary markedly with elevation in California's Sierra Nevada: precipitation increases and temperature decreases with increasing elevation [*Major*, 1988], while the natural vegetation grades from grassland to savanna to evergreen forest to dry alpine tundra [*Barbour et al.*, 2007]. The variation of easily observed ecosystem properties has been well described [*Schoenherr*, 1992]; for example, the timing of deciduous leaf out and senescence follow the thermal gradient, with broadleaves and grasses active in winter and spring at low elevation, and in summer at higher elevation. But the altitudinal patterns of other important ecosystem attributes, such as annual ET and the seasonality of evergreen-canopy gas exchange, are poorly known.

[3] Discussion of the Sierran montane climate has emphasized the limitations imposed by winter cold and summer drought [cf. *Major*, 1988; *Stephenson*, 1998; *Urban et al.*, 2000; *Royce and Barbour*, 2001a, 2001b; *Tague et al.*, 2009]. California's climate is Mediterranean, with wet winters and a long summer drought. The timing of precipitation is nearly constant with elevation, and mid-May through late October are reliably dry at all elevations, except for very infrequent and light thunderstorms. Previous analyses have suggested the growing season at mid and upper elevation is restricted to a brief window in late spring and early summer when air temperatures are warm enough for photosynthesis and soil moisture remains plentiful [*Major*, 1988; *Jeton et al.*, 1996; *Urban et al.*, 2000; *Royce and Barbour*, 2001a, 2001b; *Dettinger et al.*, 2004]. A short growing season would be expected to reduce annual transpiration, leading us to summarize current understanding with three hypotheses: (1)

[1]Department of Earth System Science, University of California, Irvine, California, USA.
[2]Now at Water Management Research, Agricultural Research Service, U.S. Department of Agriculture, Parlier, California, USA.
[3]School of Engineering, University of California, Merced, California, USA.
[4]Sierra Nevada Research Institute, University of California, Merced, California, USA.

Corresponding author: M. L. Goulden, Department of Earth System Science, University of California Irvine, CA 92697-3100, USA. (mgoulden@uci.edu)

©2012. American Geophysical Union. All Rights Reserved.
0148-0227/12/2012JG002027

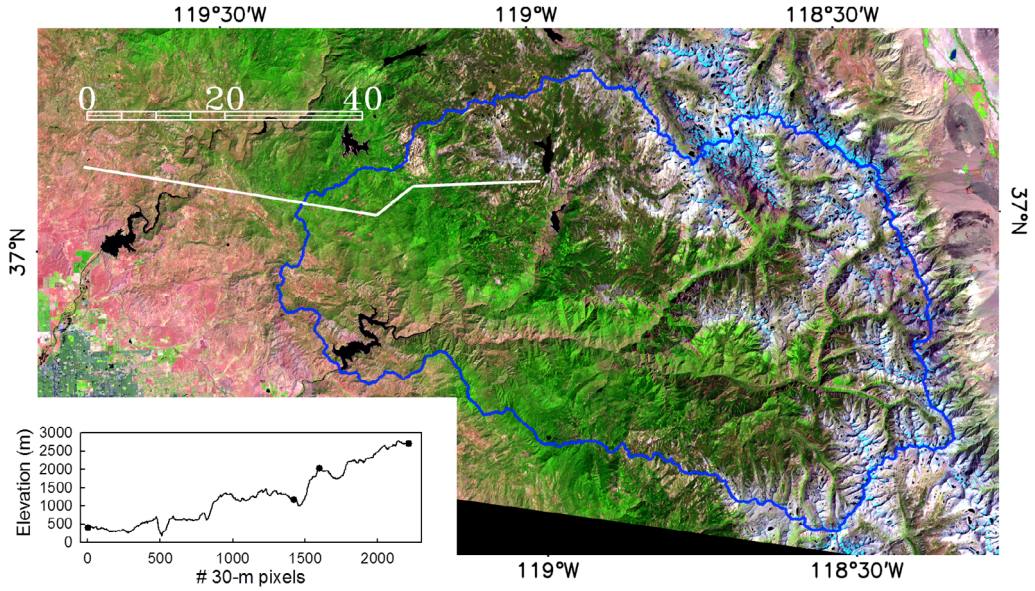

Figure 1. False color Landsat 5 Thematic Mapper image for September 4, 2011 (red is band 5, green is band 4, blue is band 3). The scale bar is km, and the blue polygon is the Upper Kings River watershed. Pine Flat Reservoir is near the southwestern edge of the watershed and the city of Fresno is in the southwestern corner of the image. The straight white lines connect the locations of the eddy covariance sites. The inset shows the elevation profiles along the segments of the eddy covariance transect.

Growing season length remains constant (or decreases) with increasing elevation due to modest increases in water availability and large increases in cold limitation. (2) The growing season is temporally offset, with a progressively later start at increasing elevation. (3) Annual ET remains constant (or decreases) with increasing elevation due to a constant (or decreasing) growing season length.

[4] Field tests of these hypotheses are infrequent and seldom span a wide elevation range. Hypotheses #1 and #2 are consistent with anecdotal visual observations of deciduous phenology. Hypothesis #2 is consistent at higher elevations with direct observations of conifer growth [*Royce and Barbour*, 2001b]. Hypothesis #2 is also supported by remotely sensed observations of deciduous phenology in Southern California's mountains [*Anderson and Goulden*, 2011]. Hypothesis #3 is consistent at higher elevations with comparisons of water balance between gauged catchments as a function of altitude [*Armstrong and Stidd*, 1967; *Lundquist and Loheide*, 2011; *Hunsaker et al.*, 2012]. But we are aware of only a few investigations that used modern plant physiological or micrometeorological methods to investigate evergreen seasonality and ET in or near the Sierra Nevada [*Royce and Barbour*, 2001a, 2001b; *Goldstein et al.*, 2000; *Ryu et al.*, 2008]. And we are unaware of any investigations that used these tools across a wide elevation range in the Sierra Nevada.

[5] An improved understanding of the patterns of phenology and ET with elevation would contribute basic knowledge on the climatic controls over ecosystem function [e.g., *Whittaker and Niering*, 1975; *Stephenson*, 1998; *Anderson-Teixeira et al.*, 2011]. Moreover, the Southwest's mountains are an important source of water, and an improved understanding of montane ET could aid near-term runoff forecasts. A better understanding of ET with elevation might also provide insight into the potential impact of climate change on regional hydrology. Assessments of western hydrological vulnerability have relied almost exclusively on land-surface models [cf. *Dettinger et al.*, 2004; *Vicuna and Dracup*, 2007]. Space-for-time substitutions, which extrapolate the current spatial relationship between climate and ecological function to future climate distribution [*Loarie et al.*, 2009], can provide information on this poorly constrained problem.

[6] We used field measurements and remote sensing to better characterize the patterns of climate, seasonality, and ET with elevation in the southern Sierra Nevada Mountains. We established and operated an eddy covariance mesonet of four matched flux towers at ~800 m elevation intervals from 405 to 2700 m elevation in and around the Upper Kings River basin. Our goals were to: (1) describe the patterns of precipitation and temperature with elevation, (2) determine how the seasonal patterns of whole ecosystem CO_2 uptake and evapotranspiration vary with elevation, precipitation, and temperature, (3) determine how annual ET varies with elevation, precipitation, and temperature, and (4) determine the influence of interannual ET variation on the patterns of Kings River discharge.

2. Methods

2.1. Study Location

[7] Our study focused on the area in and around the Upper Kings River, which drains the western slope of the Sierra Nevada east the city of Fresno, California (Figure 1). The Upper Kings watershed covers 3998 km^2 from 285 to 4313 m elevation, with a mean elevation of 2328 m. The 1971–2000 precipitation averaged over the entire watershed was 968 mm y^{-1}. The Kings drains into Pine Flat Reservoir

Table 1. Flux Tower Sites

Site Name	Dominant Vegetation	Tower Latitude	Tower Longitude	Elevation (m)	1970–99 P (mm yr^{-1})	1970–99 Min T (°C)	1970–99 Max T (°C)	MODIS Pixel Latitude	MODIS Pixel Longitude
Sierra Climate Gradient Oak/Pine Woodland	Pine, Oak, annual grass	37.1087°	−119.7313°	405 m	513 mm yr^{-1}	9.3°	23.5°	37.109°	−119.731°
Sierra Climate Gradient Ponderosa Pine Forest	Ponderosa Pine, Oak	37.0311°	−119.2563°	1160 m	805 mm yr^{-1}	5.5°	18.0°	37.031°	−119.256°
Sierra Climate Gradient Sierran Mixed Conifer Forest	White Fir, Pine, Cedar	37.0673°	−119.1948°	2015 m	1015 mm yr^{-1}	2.7°	14.8°	37.067°	−119.195°
Sierra Climate Gradient Subalpine Forest	Lodgepole Pine	37.0671°	−118.9871°	2700 m	1078 mm yr^{-1}	−1.9°	10.2°	37.067°	−118.987°
Southern California Climate Gradient Sonoran Desert	Desert perennials and annuals	33.6518°	−116.3721°	275 m	129 mm yr^{-1}	12.9°	28.8°	33.658°	−116.374°
Southern California Climate Gradient Desert Chaparral	Desert Shrubland	33.6100°	−116.4502°	1300 m	313 mm yr^{-1}	8.0°	23.6°	33.612°	−116.449°
Southern California Climate Gradient Pinyon/ Juniper Woodland	Pinyon, Juniper	33.6049°	−116.4547°	1280 m	313 mm yr^{-1}	8.0°	23.6°	33.586°	−116.461°
Southern California Climate Gradient Grassland	Annual Grassland	33.7365°	−117.6946°	470 m	408 mm yr^{-1}	9.8°	25.2°	33.756°	−117.726°
Southern California Climate Gradient Coastal Sage Shrubland	California Sage, White sage, Malosma	33.7343°	−117.6959°	475 m	408 mm yr^{-1}	9.8°	25.2°	33.755°	−117.711°
Southern California Climate Gradient Oak/Pine Forest	Oak and Pine	33.8079°	−116.7717°	1710 m	574 mm yr^{-1}	6.3°	22.0°	33.805°	−116.774°

(Figure 1). The 1971–2000 mean discharge (Q) into Pine Flat was 1.78 million acre feet y^{-1} (2.2×10^9 m^3 y^{-1}), which is equivalent to 549 mm y^{-1} averaged over the entire watershed. Water from the Kings River is fully appropriated for agricultural and urban use. The Kings River service area was home to ~750,000 people in 2003 and generated gross agricultural revenues of ~U.S.$ 3,000,000,000 [*Kings River Conservation District*, 2003].

2.2. Methodological Challenges to Understanding Montane ET

[8] The difficulty of investigating land-atmosphere exchange in mountainous terrain is widely recognized, and as a result we adopted three strategies to address or bypass the methodological challenges: (1) We relied on three types of information, micrometeorology, remote-sensing, and river flow records, which have complementary strengths and weaknesses. We used these different forms of information to independently assess the three main fluxes in the basin's hydrological balance (P, ET, and Q), and to crosscheck our approach and results at both individual sites and across the entire river basin. (2) We focused our analysis of micrometeorological observations on daytime, atmospherically unstable conditions, and avoided scientific questions that would have required accurate measures of nocturnal exchange (e.g., ones related to cumulative net CO_2 exchange). (3) We used remotely sensed observations to extrapolate in situ observations to the basin scale, and relied on an approach that did not require spatially resolved, detailed information on meteorological or soil conditions.

2.3. Eddy Covariance Measurements of CO_2 Flux and ET

[9] The accuracy of eddy covariance measurements in mountainous terrain is often questioned due to the increased likelihood of complex, 3-dimensional atmospheric flow [*Finnigan*, 2008]. These problems are most severe at night, when tall vegetation, clear nights, and topography conspire to increase cold-air drainage, causing an underestimation of ecosystem respiration and an overestimation of 24-h and longer-term carbon uptake [*Goulden et al.*, 1996, 2006; *Aubinet et al.*, 2010]. Analyses indicate daytime flux measurements in mountainous terrain are not systematically less reliable than those at comparatively flat sites [*Turnipseed et al.*, 2002, 2003]. Given the challenges of measuring nocturnal flux in the mountains, we opted to focus our analysis almost exclusively on daytime fluxes and hence ET and Gross Ecosystem CO_2 Exchange (GEE).

[10] We installed four eddy-covariance towers in and around the Upper Kings River basin during 2008 to 2010 (Figure 1 and Table 1). The sites were located along a west to east transect at ~800 m elevation intervals beginning at 405 m. All the sites were on soil developed from granitic parent material, and had vegetation that had not been disturbed recently and that was typical for the elevation. The selection of sites also weighed logistical considerations, including access, research permit availability, and micrometeorological suitability.

[11] The measurements were made near the tops of small-triangular-cross-section aluminum or steel towers that extended 5 to 10 m above the tallest trees (see *Goulden et al.* [2006] for

methodological details). Power was supplied by solar panels. The eddy covariance fluxes of CO_2 (Net Ecosystem CO_2 Exchange; NEE) and water vapor (Evapotranspiration; ET) were calculated at half hour intervals from the raw observations of wind velocity made with a sonic anemometer (Campbell Scientific CSAT-3) and CO_2 and water vapor density made with a closed-path Infrared Gas Analyzer (LiCor LI7000). Air temperature and other meteorological conditions were measured and averaged at half-hour intervals. Observations from six additional sites along a climate gradient in Southern California (Table 1) were used to establish a relationship between the Normalized Difference Vegetation Index (NDVI) and annual ET. The measurements at the Southern California sites were made and analyzed using methods that were identical to those used in the Sierras.

2.4. Calculation of Seasonal Patterns and Annual Rates of GEE and ET

[12] The half-hour eddy covariance time series were filtered to remove calm periods (observations with a friction velocity (u*) less than 0.3 m s^{-1}) [*Goulden et al.*, 1996]. The half-hourly GEE was calculated as the difference between observed NEE and the respiration determined over 30-day periods. Respiration was determined as the y-intercept of a rectangular hyperbola fit to the half hour NEEs during windy periods with incoming solar radiation (K) less than 200 Wm^{-2}.

[13] We used the energy budget closure to confirm that our daytime observations were not systematically less accurate than those reported for lowland, comparatively flat sites. The energy budget closure was determined as the linear regression forced through the origin for half-hourly observations during windy periods. The energy budget closure was 84% at the 405-m site, 75% at the 1160-m site, 85% at the 2015-m site, and 70% at the 2700-m site, which is typical of that reported for eddy covariance at comparatively more ideal sites [*Wilson et al.*, 2002; *Foken*, 2008; see also *Turnipseed et al.*, 2002, 2003]. ET and GEE were subsequently corrected for the lack of energy budget closure at each site [*Twine et al.*, 2000].

[14] Cumulative water-year (October 1 to September 30) ET and Gross Primary Production (GPP; the annual cumulative GEE) were calculated by integration after filling intervals with missing, calm, or otherwise unsuitable observations as a function of K [*Goulden et al.*, 1996, 2006; *Moffat et al.*, 2007]. Missing ET observations were filled as a linear function of K, and missing GEE as a nonlinear function of K. The incidence of missing observations varied seasonally, with more missing observations in the winter due to inadequate battery charging [*Goulden et al.*, 2006]. For example, 91% of the daylight periods in May through October 2011, and 63% of the daylight periods in January through April and November through December 2011, had usable eddy-covariance flux observations at the 2015-m site. The uncertainty associated with filling missing observations as a function of environmental conditions is typically minor [*Goulden et al.*, 1996; *Moffat et al.*, 2007], and the impact was further mitigated by the comparatively low rates of ET during the winter. The seasonal patterns of GEE and ET were determined by averaging the filled time series for individual half-hour intervals across 30-day periods and then summing over 24 h.

2.5. Species Composition and Canopy Structure

[15] Plant species composition was determined at each tower site by in situ survey in 200-m by 50-m plots oriented into the dominant wind direction, with 150-m upwind and 50-m downwind. Plant cover and canopy height were determined at each flux tower site by aircraft LIDAR in 200-m by 100-m plots oriented into the dominant wind direction, with 150-m upwind. LIDAR observations were collected by the National Center for Airborne Laser Mapping (http://www.ncalm.cive.uh.edu/) in August 2010. LIDAR observations were processed to separate 1-m resolution bare earth and first return raster images (https://snri.ucmerced.edu/CZO/data.html), and canopy height was calculated by difference. Fractional canopy cover was calculated as the proportion of pixels with a canopy height greater than 2 m.

2.6. Normal Precipitation and Air Temperature

[16] The 30-year normal precipitation and temperature was examined for the reporting weather stations on the west slope of the Sierras within 1 degree latitude and longitude of our study area (~110 km). The Normals from both the National Climate Data Center (NCDC) and the Western Regional Climate Center (WRCC) were examined, since these two sources provide slightly different types of information. The altitudinal patterns of precipitation (P) and air temperature (T) were determined with the NCDC 1981–2010 Normals, while the seasonal pattern of precipitation was determined with the WRCC 1981–2010 Normals. The length of the dry season was defined as the duration between the 95th and 5th percentiles of normal water year cumulative precipitation. Both sets of normals were obtained from the WRCC (http://www.wrcc.dri.edu/Climsum.html; NCDC Normals downloaded Nov. 21, 2011; WRCC Normals downloaded Dec. 1, 2011). There was partial but not complete overlap between the sites used for the NCDC and WRCC analyses. The following stations were used for either or both analyses: Ash Mountain, Auberry 1 Northwest, Balch Power House, Big Creek Phase 1, Cherry Valley Dam, Corcoran Irrigation District, Coarsegold 1 Southwest, Five Points 5 Southsouthwest, Fresno Yosemite Airport, Friant Government Camp, Grant Grove, Hanford 1 South, Hetch Hetchy, Huntington Lake, Lemon Cove, Lindsay, Lodgepole, Madera, Meadow Lake, North Fork Ranger Station, Pine Flat Dam, South Entrance Yosemite National Park, Visalia, Yosemite Park Headquarters.

2.7. Extrapolating ET With Remote Sensing

[17] Many approaches are available to spatially extrapolate ET based on remotely sensed observations [*Li et al.*, 2009; *Glenn et al.*, 2008]. These strategies may be divided into two categories: (1) Physically based methods, which use either remotely sensed surface temperature and an analysis of the surface energy budget [e.g., *Bastiaanssen*, 2000], or reflectance-derived surface biophysical properties and an approach such as the Penman–Monteith equation [e.g., *Mu et al.*, 2011]. (2) Regression methods, which directly apply an empirical relationship between remotely sensed Vegetation Indices (VIs) and observations of ET [*Glenn et al.*, 2010].

[18] In the long term, many researchers feel physically based ET methods will prove superior, since they have a strong theoretical basis and, given an accurate representation

of the surface, provide an accurate extrapolation of ET. In the short term, physically based approaches are subject to disadvantages that may limit their usefulness in mountainous terrain. Physically based approaches require spatially resolved meteorological inputs, such as radiation, temperature, humidity, wind speed, and precipitation, which may vary markedly over small distances with elevation and aspect. Extrapolation of montane meteorological conditions to fine scale may be highly uncertain due to this heterogeneity, as well as inadequate understanding of montane boundary layer development and sparse in situ meteorological data. Similarly, soil conditions may be poorly characterized in the mountains, and properties such as soil water holding capacity and rooting depth may vary markedly with topography.

[19] Regression approaches do not require inputs beyond the observed VIs, and are not impacted by the lack of accurate spatially resolved meteorological and soil information. Moreover, several considerations call into question the assumption that physically based strategies are inherently better than regression approaches. ET algorithms are subject to equifinality constraints [*Beven*, 2006]; complex approaches will not necessarily outperform simple, regression strategies [*Glenn et al.*, 2010]. Additionally, feedbacks associated with resource optimization theory [*Field*, 1991] may cause a stronger relationship between a VI and ET than could be predicted based solely on the physical controls on ET [*Glenn et al.*, 2010]. In semi-arid regions, a site's water balance, Leaf Area Index (LAI), primary production, and annual ET are tightly correlated through a series of feedbacks [*Grier and Running*, 1977; *Gholz*, 1982]. A high LAI both drives a high annual ET and is symptomatic of a location with a high ET. In turn, LAI is well correlated with the Normalized Vegetation Difference Index (NDVI) [*Carlson and Ripley*, 1997], creating a tight relationship between NDVI and ET. Previous studies have confirmed an extraordinarily strong correlation between annual ET and NDVI across semi-arid landscapes [*Groeneveld et al.*, 2007].

[20] Based on these considerations, we investigated the relationships between annually integrated eddy-covariance ET and observations collected by the MODerate resolution Imaging Spectroradiometer (MODIS). We compared tower-based ET to the annually integrated MODIS ET product (MOD16A2 Collection 5) [*Mu et al.*, 2011], the snow-free annual average NDVI (MYD13Q1 Collection 5) [*Huete et al.*, 2002], and the snow-free average Enhanced Vegetation Index (EVI). MOD13 and MOD16 time series were downloaded from the Oak Ridge National Laboratory Distributed Active Archive Center for Biogeochemical Dynamics (ORNL DAAC; http://daac.ornl.gov/MODIS/; downloaded Feb. 24, 2012). The area of homogenous vegetation around the flux tower at some sites was too small to provide a reliable MODIS target, and MODIS observations for a nearby, larger patch of similar vegetation were used in these cases (i.e., the MODIS pixels in Table 1). The 16-day MOD13 and 8-day MOD16 data were downloaded for each tower's MODIS pixel and summed or averaged for each water year.

[21] We found annually integrated MOD16 was poorly correlated with in situ ET, especially for montane forest (Figure 2a). The magnitude of MOD16 ET averaged across all the sites was in rough agreement with the average observed in situ. But the sites with the highest in situ ET (Oak/pine forest and Sierra mixed conifer forest) had comparatively low rates of MOD16 ET. The poor agreement presumably reflects erroneous meteorological or biogeophysical inputs to the MOD16 algorithm. Given that similar inputs are required for other physically based ET approaches, and that the development of spatially resolved meteorological or soil inputs in montane landscapes is particularly challenging, we conclude additional evaluation is needed before these methods can be reliably applied to the Sierra Nevada.

[22] In contrast, the much simpler approach of regressing a VI against in situ ET performed well. Both NDVI and EVI were well correlated with ET, with a marginally tighter correlation observed for NDVI ($r^2 = 0.9154$; Figure 2b). The montane sites (Oak/pine forest, Ponderosa pine forest, Sierra mixed conifer forest, and Subalpine forest) were not anomalous relative to the lowland sites. Both VIs saturated at high ET, where incremental increases in ET were associated with progressively smaller increases in NDVI or EVI. Neither VI responded consistently to the reduced rates of ET in 2007, which was an extraordinarily dry year. Moreover, we emphasize that our regression approach is unsuitable for quantifying the day-to-day or seasonal patterns of ET, when meteorological conditions and plant phenology play dominant roles, and a more physically based approach is required.

2.8. Spatial Patterns of P, ET, and P-ET

[23] We combined existing spatially resolved information on precipitation with MODIS NDVI observations to estimate the P, ET and P-ET for the entire Upper Kings watershed. Gridded monthly P calculated using the Parameter-elevation Regressions on Independent Slopes Model (PRISM) was obtained for 2002 to 2010 at 2.5-arcmin (0.04167°; ~4 km) resolution, and for the 1971 to 2000 normal at 30-arcsec (0.0083°; ~800 m) resolution [*Daly et al.*, 1994] (PRISM Climate Group, Oregon State University; http://prism.oregonstate.edu, downloaded Nov. 9, 2011). The monthly 2.5-arcmin PRISM images were then summed for each water year (October to September).

[24] Gridded ET was calculated from the water-year mean NDVIs obtained by the Aqua satellite MODIS. MODIS imagery for the Kings River watershed was obtained from the ORNL DAAC (http://daac.ornl.gov/MODIS/; MYD13Q1 Collection 5; in geographic coordinates at 0.002083° resolution, downloaded Oct. 16, 2011). NDVI data were filtered to include only the highest quality observations (pixel reliability = 0) for day of (calendar) year (DOY) 0–201 and 265–365. A pixel reliability of 0 or 1 was used for DOY 201–265 (these late summer periods were reliably cloud free and largely snow free). NDVI was averaged for each water year, and ET was calculated based on the regression between annual NDVI and ET (Figure 2b). The relationship between NDVI and ET is almost certainly driven by the transpirational component of ET [*Glenn et al.*, 2010], and it will underestimate ET for evaporation-dominated locations, such as lakes or reservoirs, and possibly also sublimation-dominated locations.

[25] Gridded P-ET was calculated by difference between P and ET on a pixel by pixel basis at 0.002083° resolution. Annual runoff was calculated for individual water years using the corresponding 2.5-arcmin PRISM records. All spatial analyses were done for the entire Upper Kings River

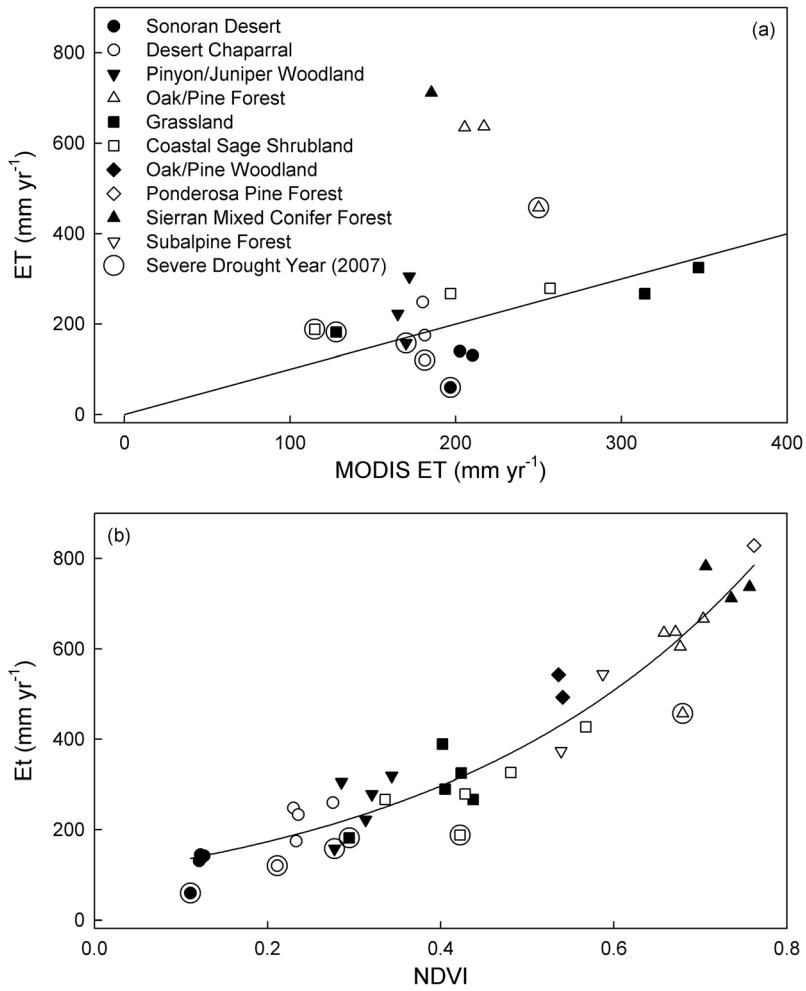

Figure 2. (a) Annual total ET (mm yr^{-1}) across 8 sites and 19 site years as a function of annual mean integrated water year ET based on the MODIS ET product (MOD16; (MOD16 was unavailable for 2010 and 2011 water years); solid line indicates 1:1). (b) Annual total ET (mm yr^{-1}) across 10 sites and 37 site years as a function of annual mean Normalized Difference Vegetation Index (NDVI; dimensionless). Drought years (circled) are 2007 for Southern California sites, when Precipitation was extraordinarily low. The best fit regression for all years was ET = 101.49 * $e^{(2.6853*NDVI)}$ (R^2 = 0.9154).

watershed, as demarcated by the United States Geologic Survey 8 Digit Watershed Boundary Data set (http://datagateway.nrcs.usda.gov/; downloaded April 6, 2011). Elevation was based on the National Elevation Data set at 30-m resolution obtained from the U.S. Department of Agriculture Natural Resources Conservation Service Geospatial Data Gateway (http://datagateway.nrcs.usda.gov/; downloaded April 7, 2011). The spatially gridded P, ET, and P-ET were subsequently divided into 200-m elevation bins and the corresponding minimum, maximum, mean, and standard deviation calculated.

[26] We did not attempt a rigorous uncertainty analysis of NDVI-based ET, PRISM P, or P-ET. It is unlikely the uncertainty of either P or ET is less than ±10 to 15%, given the variety of possible errors. The uncertainty of P-ET is probably greater, since it is the residual of larger terms.

[27] The interannual patterns of water year P, ET, and P-ET averaged across the entire watershed were compared with the unimpaired runoff into Pine Flat Reservoir summed for corresponding periods. The Pine Flat inflow record was obtained from the California Data Exchange Center (http://cdec.water.ca.gov/; Kings River - Pine Flat Dam Full Natural Flow; downloaded Nov. 10, 2011).

3. Results

3.1. Altitudinal Patterns of Climate and Vegetation

[28] The Kings basin experiences a montane Mediterranean climate; more than 90% of precipitation falls from late October to mid-May and the summer is reliably dry (WRCC Normals; data not shown). Most of the precipitation occurs during large frontal storms that move off the Pacific Ocean from west to east. Precipitation increases rapidly with elevation to ~500 m, and more gradually at higher elevations (NCDC Normals; plot not shown; P(mm) = 107.7 + 1338 * (elevation(m)/(656 + elevation(m)); r^2 = 0.947). The period without appreciable precipitation is slightly longer at lower elevations, which may remain dry during weak late-season storms. On average, a site at 400-m elevation has a 172-day dry season and a site at 2000 m has a 156-day dry season

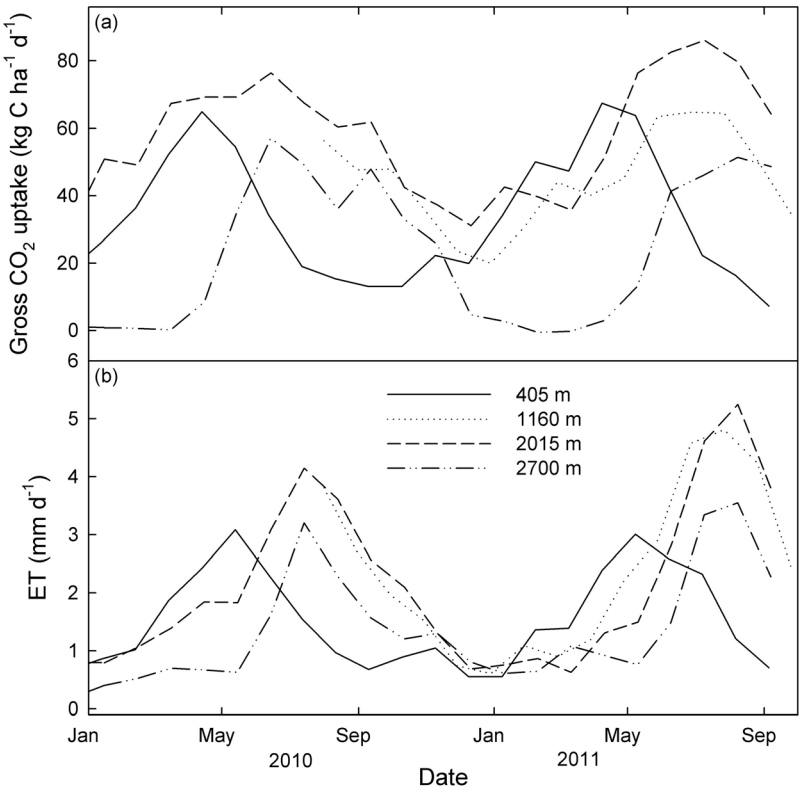

Figure 3. Seasonal patterns of (a) gross CO_2 uptake (GEE) and (b) ET at the flux tower sites. Lines connect averages at 30-day intervals.

(WRCC Normals; data not shown). Areas above 2500 m receive most precipitation as snow; areas from 1500 to 2500 m receive a mix of snow and rain; areas below 1500 m receive mostly rain [*Bales et al.*, 2011].

[29] The daily mean air temperature at the top of the 2015-m tower was 2.6°C in winter and 17.2°C in summer. The seasonality of temperature was independent of elevation: the temperature at all sites varied in parallel, indicating a nearly constant atmospheric lapse rate. The average atmospheric lapse between the eddy covariance towers was -5.3°C km^{-1} in 2011 (plot not shown; Tower T (°C) = -0.00530 * elevation (m) + 20.21; $R^2 = 0.999$). The lapse calculated from the NCDC Normals was -5.1°C km^{-1} (Normal T (°C) = -0.00510 * elevation (m) + 18.28; $R^2 = 0.946$).

[30] Large changes in vegetation type and density occurred with elevation (data not shown). The 405-m site was an open savanna with a continuous cover of annual grasses and 25% pine and oak cover. The 1160-m site was a lower montane forest with 63% ponderosa pine and oak cover. The 2015-m site was a mid-montane forest with 53% white fir and pine cover. The 2700-m site was an open subalpine forest with 31% lodgepole pine cover.

3.2. Seasonal Patterns of Canopy Gas Exchange With Altitude

[31] Gross Ecosystem CO_2 Exchange (GEE) is a measure of whole-forest photosynthesis; increasing GEE indicates increasing photosynthesis (Figure 3a). GEE at 405 m peaked in late spring (March to May) and declined markedly in summer (July to September). GEE at mid-elevation (1160 and 2015 m) continued year-round, with modest declines during the winter (November to March) and late drought (September to October). GEE at 2700 m peaked in summer and early fall (May to October) and ceased in winter and early spring. ET represents the sum of transpiration, evaporation, canopy interception and sublimation. Transpiration is tightly linked with GEE through leaf gas exchange, and the seasonal ET differences with elevation were similar to, though less pronounced than, the patterns observed for GEE (Figure 3b).

[32] The seasonal patterns and rates of ET and GEE were generally similar between 1160 and 2015 m despite a large difference in precipitation form. Both sites showed year-round gas exchange despite a transition from rain dominated precipitation at 1160 m and the absence of a lasting snowpack, to mixed precipitation at 2015 m and a snowpack that often lasted until late May.

[33] A phenological threshold occurred between 2015 m, where CO_2 uptake continued year-round, and 2700 m, where CO_2 uptake ceased in winter (Figure 3a). This shift was associated with the development of plant dormancy and not the immediate limitation of cold on leaf gas exchange (Figure 4). The net CO_2 uptake at 2700 m during well-illuminated winter periods was consistently negative (i.e., a net loss of CO_2 to the atmosphere). The site did not have an appreciable photosynthesis rate during the winter, even on unusually warm days. In contrast, the 2015-m site remained capable of photosynthesis throughout the winter. The net CO_2 uptake at 2015 and 2700 m showed similar temperature dependence in summer. The transition from a year-round growing season at 2015 m to winter dormancy at 2700 m coincided with a between-site mean daytime temperature difference of 3.8°C (Figure 4).

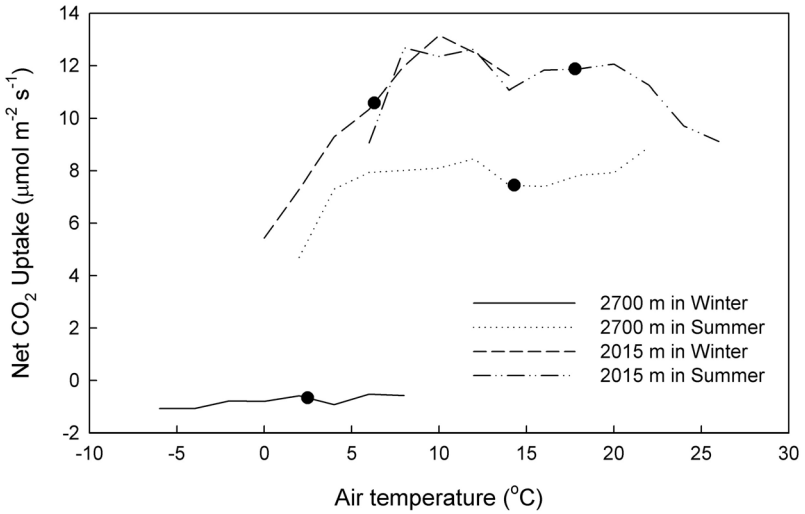

Figure 4. Relationship between air temperature and net ecosystem CO_2 uptake (lines connecting averages for 2° bins; positive fluxes indicate greater ecosystem CO_2 uptake) during sunny (incoming solar radiation greater than 200 W m^{-2}) winter (December 10 through March 30) and summer (June 8 through November 20) periods at the two highest elevation sites. The filled circles indicate the mean air temperature at each site during sunny periods in the corresponding season.

3.3. Altitudinal Patterns of ET

[34] Annual ET measured by eddy covariance was greatest at 1160 and 2015 m, and was 35% lower at 405 m coincident with less P, and 40% lower at 2700 m coincident with colder temperatures (Figure 5). Gross Primary Production showed a similar trend with elevation, as would be expected based on the tight leaf-level coupling between transpiration and photosynthesis [*Chapin et al.*, 2002].

3.4. Altitudinal Patterns of ET and P-ET by Remote Sensing

[35] PRISM Precipitation was well correlated with elevation, showing a strong increase from west to east with increasing altitude (Figures 6a and 6b). PRISM precipitation was reduced in some of the eastern sections of the watershed, even at higher elevation, presumably because of rain shadowing. We combined the empirical NDVI-ET relationship (Figure 2b) with MODIS imagery to calculate gridded records of annual ET for 2003 to 2011 over the entire Upper Kings watershed (Figure 6c). NDVI-based ET peaked at mid-elevation, with moderately high ET at the lowest elevations in the western part of the basin and very low rates of ET in the highest, eastern regions. We combined ET on a pixel by pixel basis with the corresponding precipitation based on the PRISM approach (Figure 6b) to calculate P-ET (Figure 6d). P-ET was consistently low in the western, lower parts of the basin, and greatest in the eastern, high elevation reaches.

[36] P-ET extrapolated to the entire watershed agreed remarkably well with the corresponding discharge (Q) into

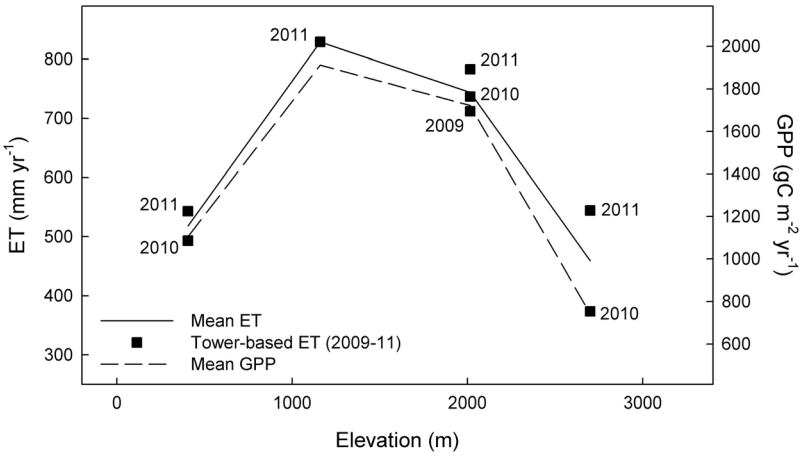

Figure 5. Relationships between elevation, evapotranspiration (ET; mm y^{-1}; filled squares show values for individual water years and solid lines connect averages), and gross primary production (GPP; gC m^{-2} y^{-1}; positive fluxes indicate CO_2 uptake by the land surface; dashed lines connect averages) determined by annually summing GEE.

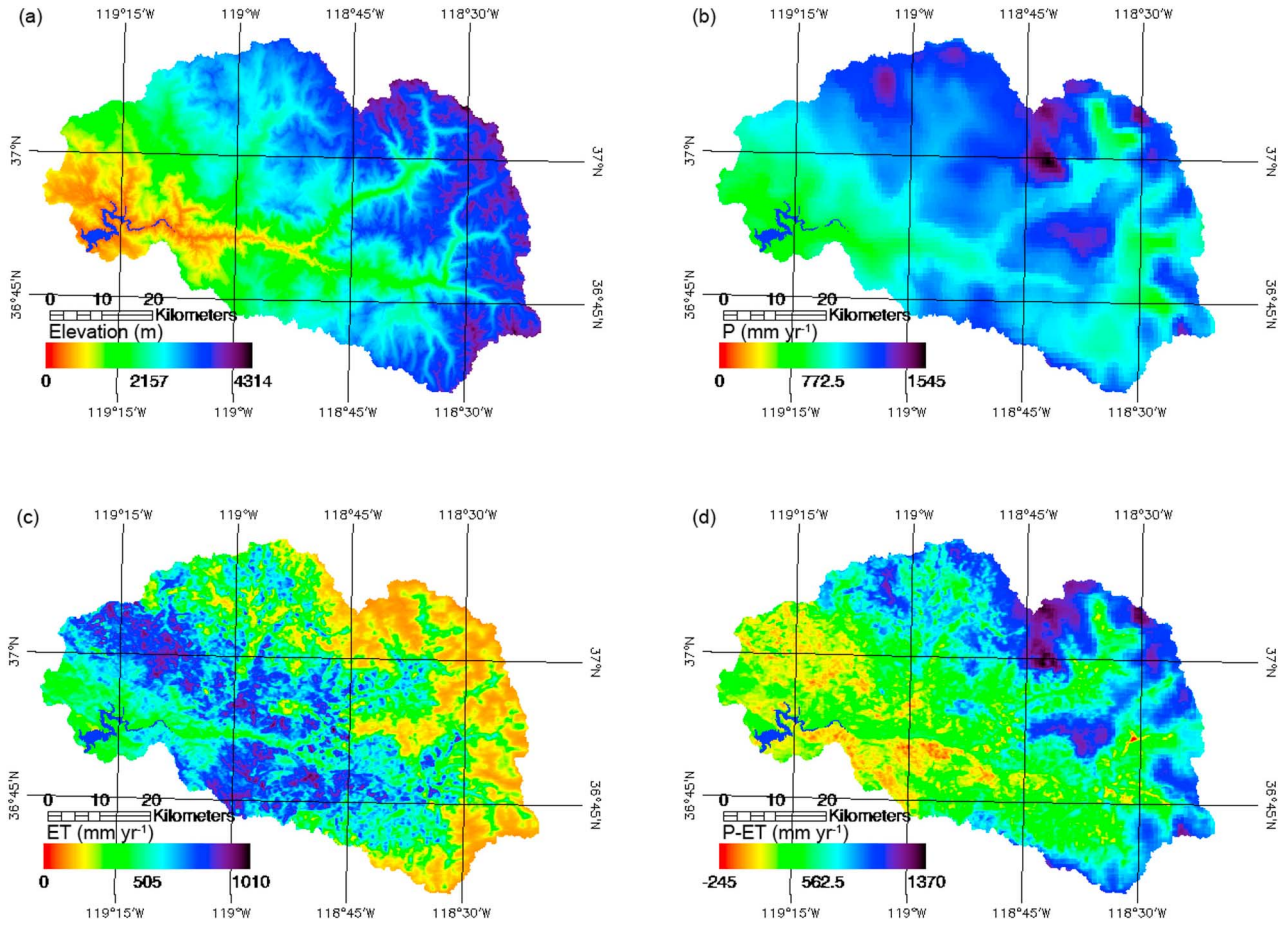

Figure 6. Upper Kings River basin with Pine Flat Reservoir (in blue) at the southwestern edge. (a) Elevation in m above sea level (0 m in red to 4314 m in dark violet). (b) Precipitation 30-year climatology (1971 to 2000 PRISM Normal; 0 mm y^{-1} in red to 1545 mm y^{-1} in dark violet). (c) Average (2003 to 2011) evapotranspiration calculated from NDVI (0 mm y^{-1} in red to 1010 mm y^{-1} in dark violet). (d) P-ET calculated as Figure 6b minus Figure 6c (−245 mm y^{-1} in red to 1370 mm y^{-1} in dark violet).

Pine Flat Reservoir (Figure 7), though this may be partly fortuitous given the uncertainty in P-ET. The mean 2003–11 P for the entire watershed was 984 mm y^{-1} and the mean ET based on NDVI was 429 mm y^{-1}, yielding a P-ET of 554 mm y^{-1}, which is quite close to the 2003–11 full natural flow into Pine Flat of 563 mm y^{-1}. The NDVI-based ET was nearly constant from year to year, ranging from 413 mm y^{-1} in 2008, which was a drier than average year following an extraordinarily dry year, to 451 mm y^{-1} in 2011, which was a very wet year following a wetter than average year. The interannual patterns of ET were similar to those observed at the 2015-m flux tower site. ET at 2015 m increased 8% from 2009 to 2011 (Figure 5) coincident with increasing P (Figure 7), while NDVI-based ET for the entire basin increased 9% (Figure 7).

[37] The NDVI-based ET showed an altitudinal pattern that was similar to that observed in situ (Figures 8 and 5). NDVI-based ET peaked at 1600 to 1800 m and was reduced at both higher and lower elevation. The PRISM-based P showed a steady rise with elevation, with some leveling off in the 2000 to 3500-m range, and an increase in P at the highest elevations. The P at these highest elevations is very uncertain due to a lack of observations, though this uncertainty is unlikely to affect our analysis since this elevation accounts for a small fraction of the watershed. P and ET increased in tandem up to 1700 m, resulting in a low and constant P-ET. P-ET increased by 660 mm y^{-1} from 1700 m to 3500 m, with 80% of this increase attributable to declining ET and the remaining 20% to increasing P.

4. Discussion

4.1. Crosschecks

[38] Montane landscapes provide one key advantage for investigating large-scale hydrology. The lower boundary of montane watersheds is often well-sealed, which limits discharge to groundwater. Additionally, the rate of surface flow is often well characterized using river gauges and reservoir level. Discharge to groundwater in the Upper Kings River basin is thought to be minor, as a result of the underlying granite batholith. Our strategy allowed a series of cross-comparisons between largely independent measures. In particular, we were able to: (1) Confirm that eddy-covariance and remote-sensing provided qualitatively similar patterns of ET with elevation (Figures 5 and 8). (2) Confirm that total ET calculated for the Upper Kings Basin based on

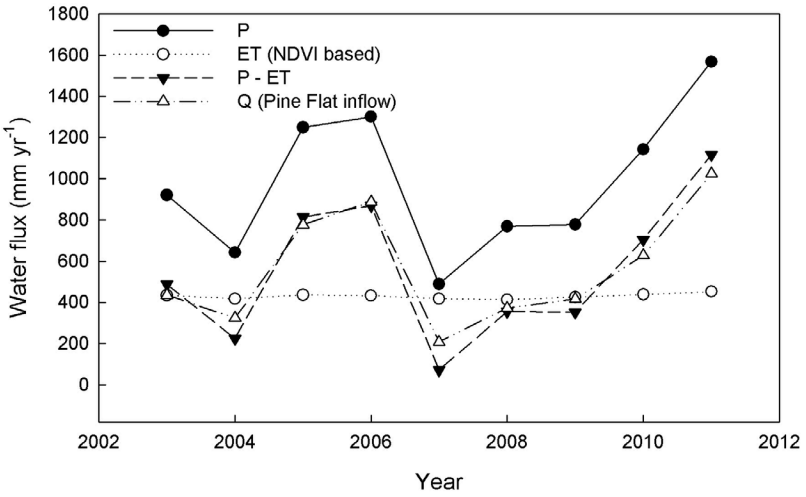

Figure 7. Interannual variability of water balance for the entire Upper Kings River watershed. Plot shows precipitation (mm y^{-1}; filled circles; integrated PRISM monthly values), evapotranspiration (ET; mm y^{-1}; open circles; based on regression between ET and the Normalized Difference Vegetation Index), the difference between P and ET (mm y^{-1}; inverted filled triangles), and the observed discharge (Q) into Pine Flat Reservoir (mm y^{-1}; open triangles). The time series were calculated by summing annually resolved raster values similar to those in Figure 6 for individual water years.

remote sensing was quantitatively similar to that calculated by the difference between P and Q (Figure 7). (3) Confirm that interannual ET variability calculated for the Upper Kings Basin based on remote sensing was qualitatively similar to that calculated for the basin by the difference between P and Q (Figure 7). The crosschecks markedly increased our confidence in the results.

4.2. Patterns of Climate and Seasonality With Elevation

[39] The altitudinal patterns of precipitation, temperature, plant species composition, and vegetation structure were similar to previous reports [*Major*, 1988; *Urban et al.*, 2000; *Barbour et al.*, 2007]. Precipitation increased rapidly with elevation to ~500 m (NCDC and WRCC Normals), and more gradually at higher elevations (NCDC and WRCC Normals; Figure 8), a pattern typical of the Sierra Nevada [*Major*, 1988; *Armstrong and Stidd*, 1967]. Likewise, the relatively shallow atmospheric lapse rate (-5.3°C km^{-1}) is similar to that reported previously for the area [*Major*, 1988].

[40] Our observations of the seasonality and duration of CO_2 uptake and ET provide evidence that the first two hypotheses are over simplifications. We found that growing season length increased from 405 m to 1160 m, and that mid-elevation sites were photosynthetically active year-

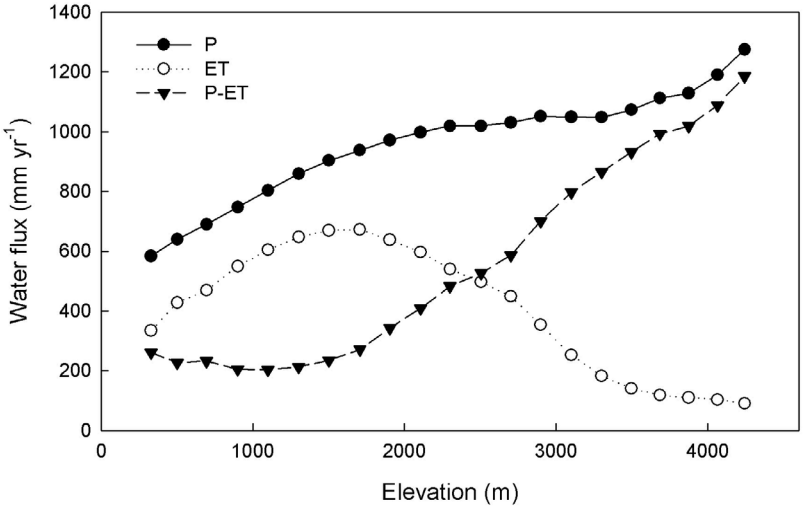

Figure 8. Relationships between elevation and P (mm y^{-1}; filled circles; 1971 to 2000 PRISM Normal), ET (mm y^{-1}; open circles; 2003 to 2011 NDVI-based regression), and P-ET (mm y^{-1}; inverted filled triangles; calculated). The elevation trends were calculated by binning and averaging the raster values in Figure 6.

round (Figures 3 and 4), contradicting Hypothesis #1 (growing season length remains constant (or decreases) with increasing elevation), with the main discrepancy a result of the year-round growing season at mid-elevation. Likewise, we found high rates of CO_2 uptake earlier in the water year at mid-elevation than at low elevation (Figure 3), contradicting Hypothesis #2 (the growing season is temporally offset, with a progressively later start at increasing elevation), with the main discrepancy again at mid-elevation. The year-round growing season at mid-elevation reflected two phenomena that we feel have been underappreciated: the mid-elevation sites experienced only minor cold limitation in winter, and the mid-elevation sites largely escaped summer drought.

[41] The lack of strong cold limitation at 2015 m is attributable to physiological adaptations or acclimations that allow high rates of evergreen photosynthesis at an air temperature of just 5°C (Figure 4). The forest at 2015 m maintained higher rates of photosynthesis at lower temperatures than have been reported for other evergreen forests [*Yuan et al.*, 2011], and also than would be expected based on a commonly used parameterization for photosynthesis [*Farquhar et al.*, 1980]. Previous discussions failed to appreciate the potential for high rates of photosynthesis within just a few degrees of freezing (but see *Waring and Franklin* [1979]), and may have misinterpreted the presence of a deep snowpack and deciduous leaf drop at mid-elevation as evidence of evergreen dormancy.

[42] The phenological transition from winter-active evergreens at 2015 m elevation to winter-dormant evergreens at 2700 m coincided with a reduction in mean daytime temperature of 3.8°C (Figure 4). The phenological transition was accompanied by an almost complete turnover of plant species composition. The marked species turnover in this elevation range has been described before and attributed to the location of the mean storm snowline [*Barbour and Minnich*, 2000; *Royce and Barbour*, 2001a, 2001b]. We propose an alternative hypothesis: the modest winter daytime temperature decline from 6.3°C at 2015 m to 2.5°C at 2700 m crossed the threshold between a climate that favored winter activity and one that favored dormancy (Figure 4). This caused a large turnover of canopy species composition, with a shift from winter active species such as white fir to winter dormant species such as lodgepole pine.

[43] The lack of strong drought limitation at the mid-elevation sites was not attributable to water storage in the snowpack; we did not observe a major difference in seasonality between 1060 and 2015 m despite a large difference in precipitation form and snowpack duration. Instead, we attribute the lack of mid-elevation drought limitation to deep rooting. Less than 2 mm of precipitation fell near the 2015-m site during a 154-day period in summer 2010, and the 464 mm cumulative ET during this period (Figure 3) was withdrawn from the soil. The soil at 2015-m was coarse, and plant available water was 0.10 to 0.20 $cm^3\ cm^{-3}$ [*Bales et al.*, 2011], implying a rooting depth of 2.5 to 5 m. The importance of deep rooting is well known for California ecosystems such as chaparral and oak woodland [*Hellmers et al.*, 1955; *Griffin*, 1973; *Goulden*, 1996], and it comes as no surprise that montane forest relies on a similar strategy [*Arkley*, 1981; *Hubbert et al.*, 2001; *Rose et al.*, 2003].

4.3. Interannual Patterns of Kings River Basin P, ET, P-ET, and Q

[44] Watershed ET was comparatively constant from year to year; P drove interannual P-ET variability, with modest hysteresis presumably caused by interannual soil storage changes (Figure 7). The dominance of interannual P as a driver of interannual Q, and the finding that interannual Q variation is proportionally greater than interannual P variation, were previously recognized [*Risbey and Entekhabi*, 1996].

[45] The consistency of Upper Kings basin ET from year to year is supported by three pieces of evidence: the tower-based ET at 2015 m was similar across the three years of observations (Figure 5); the NDVI-based calculations of ET varied little from year to year (Figure 7), and the difference between PRISM P and Pine Flat Q was relatively constant from year to year (Figure 7) [see also *Lundquist and Loheide*, 2011]. The Upper Kings water balance may be summarized with a few simple hypotheses. ET varies little from year to year despite large P variation. The interannual ET constancy may be attributed in part to deep rooting, which allows montane vegetation access to large soil water reservoirs and buffers interannual P variability. Interannual Q variation is closely related to P-ET variation, with modest hysteresis associated with changes in soil water storage. The constancy of ET amplifies the effect of P variation on Q, such that the proportional change in P-ET between years is greater than the proportional change in P alone.

4.4. Patterns of ET With Elevation

[46] Annual ET measured by eddy covariance and also calculated from NDVI showed a peaked distribution, with a maximum at mid-elevation and declines at high and low elevation (Figures 5 and 8). The declining ET above 2015 m is consistent with the decreasing P-Q reported at higher elevations in the American [*Armstrong and Stidd*, 1967], Merced [*Lundquist and Loheide*, 2011], and Kings [*Hunsaker et al.*, 2012] River basins in the Sierra Nevada. We are unaware of comparable analyses of the altitudinal dependence of P-Q at lower elevations with which to compare our observations. The increase in ET from 405 to 1160 m elevation indicates that Hypothesis #3 (annual ET remains roughly constant (or decreases) with increasing elevation due to a constant (or decreasing) growing season length) is an oversimplification. The peaked shape of ET and GPP with elevation parallels growing season length; growing season was longest at mid-elevation (Figure 3). The divergence between our findings (Figure 5) and the premise of a systematically decreasing ET with elevation (Hypothesis #3) reflects previous expectation that both cold and drought curtail mid-elevation gas exchange.

[47] The density and stature of the vegetation and the maximum rates of CO_2 uptake and ET in summer were all greatest at mid-elevation (Figure 5). We suspect these trends reflect slow, biological feedbacks between GPP and canopy structure that amplify the effect of growing season length on gas exchange. The climatic conditions at mid-elevation allow year-round photosynthesis, which results in increased GPP and allocation to plant growth. Increased plant growth results in a higher Leaf Area Index (LAI) and possibly increased root density, which should enhance mid-summer

CO_2 uptake. The limitations imposed by drought at lower elevations and cold at higher elevations result in negative feedbacks that decrease LAI. Hence, we expect many ecosystem properties will also show a peaked pattern with elevation, in part due to feedbacks that amplify the physical climatic constraints [*Chapin et al.*, 2002].

[48] The sharp drop-off in ET above 2000 m was attributed to the phenological transition to winter dormancy with moderately colder winter temperatures, and associated feedbacks that decrease plant density and LAI. This threshold raises the possibility of a large increase in ET in the 2000 to 3000 m range with climate change. The climate in the southern Sierra Nevada is projected to warm 3°C by 2070–99 [*U.S. Bureau of Reclamation*, 2011]. The atmospheric lapse around the Kings was $-5.3°\ km^{-1}$, and a 3°C warming could move the steady state vegetation distribution upslope by 550 to 600 m, assuming the biogeography is controlled exclusively by temperature. Climatic warming at 2700 m would be expected to decrease the local limitation imposed by cold, and expand the growing season length (Figures 3 and 4). Species already at the site that are able to capitalize on warmer winter temperatures may increase in importance, and species that are currently restricted to lower elevations may become established. With time, species composition would be expected to shift toward plants that are capable of a year-round growing season, and the density of the canopy (LAI) would be expected to increase. The vegetation at 2700 m may ultimately resemble that currently found at 2015 m, with a corresponding local ET increase of up to 60% (Figure 5) and a concomitant decrease in P-ET (Figure 8).

[49] **Acknowledgments.** Research was supported by the U.S. National Science Foundation, through the Southern Sierra Critical Zone Observatory (EAR-0725097) and a Major Research Instrumentation grant (EAR-0619947), and by the U.S. Department of Energy Terrestrial Ecosystem program. The Sierra Nevada Eddy Covariance sites were located at the San Joaquin Experimental Range, the King River Experimental Watershed, and on the Sierra National Forest in cooperation with the United States Forest Service.

References

Anderson, R., and M. Goulden (2011), Relationships between climate, vegetation, and energy exchange across a montane gradient, *J. Geophys. Res.*, *116*, G01026, doi:10.1029/2010JG001476.

Anderson-Teixeira, K. J., J. P. Delong, A. M. Fox, D. A. Brese, and M. E. Litvak (2011), Differential responses of production and respiration to temperature and moisture drive the carbon balance across a climatic gradient in New Mexico, *Global Change Biol.*, *17*(1), 410–424, doi:10.1111/j.1365-2486.2010.02269.x.

Arkley, R. J. (1981), Soil-moisture use by mixed conifer forest in a summer-dry climate, *Soil Sci. Soc. Am. J.*, *45*(2), 423–427, doi:10.2136/sssaj1981.03615995004500020037x.

Armstrong, C. F., and C. K. Stidd (1967), A moisture balance profile on the Sierra-Nevada mountains California USA, *J. Hydrol.*, *5*(3), 258–268, doi:10.1016/S0022-1694(67)80105-7.

Aubinet, M., C. Feigenwinter, B. Heinesch, C. Bernhofer, E. Canepa, A. Lindroth, L. Montagnani, C. Rebmann, P. Sedlak, and E. Van Gorsel (2010), Direct advection measurements do not help to solve the night-time CO_2 closure problem: Evidence from three different forests, *Agric. For. Meteorol.*, *150*(5), 655–664, doi:10.1016/j.agrformet.2010.01.016.

Bales, R. C., J. W. Hopmans, A. T. O'Geen, M. Meadows, P. C. Hartsough, P. Kirchner, C. T. Hunsaker, and D. Beaudette (2011), Soil moisture response to snowmelt and rainfall in a Sierra Nevada mixed-conifer forest, *Vadose Zone J.*, *10*(3), 786–799, doi:10.2136/vzj2011.0001.

Barbour, M. G., and R. A. Minnich (2000), California upland forests and woodlands, in *North American Terrestrial Vegetation*, edited by M. G. Barbour and W. D. Billings, pp. 161–202, Cambridge Univ. Press, Cambridge, U. K.

Barbour, M. G., T. Keeler-Wolf, and A. A. Schoenherr (2007), *Terrestrial Vegetation of California*, 3rd ed., 730 pp., Univ. of Calif. Press, Berkeley, doi:10.1525/california/9780520249554.001.0001.

Bastiaanssen, W. G. M. (2000), SEBAL-based sensible and latent heat fluxes in the irrigated Gediz Basin, Turkey, *J. Hydrol.*, *229*(1–2), 87–100, doi:10.1016/S0022-1694(99)00202-4.

Beven, K. (2006), A manifesto for the equifinality thesis, *J. Hydrol.*, *320*(1–2), 18–36.

Carlson, T. N., and D. A. Ripley (1997), On the relation between NDVI, fractional vegetation cover, and leaf area index, *Remote Sens. Environ.*, *62*(3), 241–252, doi:10.1016/S0034-4257(97)00104-1.

Chapin, F. S. I., P. A. Matson, and H. A. Mooney (2002), *Principles of Terrestrial Ecosystem Ecology*, 436 pp., Springer, New York.

Daly, C., R. P. Neilson, and D. L. Phillips (1994), A statistical topographic model for mapping climatological precipitation over mountainous terrain, *J. Appl. Meteorol.*, *33*(2), 140–158, doi:10.1175/1520-0450(1994)033<0140:ASTMFM>2.0.CO;2.

Dettinger, M. D., D. R. Cayan, M. Meyer, and A. E. Jeton (2004), Simulated hydrologic responses to climate variations and change in the Merced, Carson, and American River basins, Sierra Nevada, California, 1900–2099, *Clim. Change*, *62*(1–3), 283–317, doi:10.1023/B:CLIM.0000013683.13346.4f.

Farquhar, G. D., S. V. Caemmerer, and J. A. Berry (1980), A biochemical-model of photosynthetic CO_2 assimilation in leaves of C-3 species, *Planta*, *149*(1), 78–90, doi:10.1007/BF00386231.

Field, C. B. (1991), Ecological scaling of carbon gain to stress and resource availability, in *Response of Plants to Multiple Stresses*, edited by H. A. Mooney, W. E. Winner, and E. J. Pell, pp. 35–65, Academic, San Diego, Calif.

Finnigan, J. (2008), An introduction to flux measurements in difficult conditions, *Ecol. Appl.*, *18*(6), 1340–1350, doi:10.1890/07-2105.1.

Foken, T. (2008), The energy balance closure problem: An overview, *Ecol. Appl.*, *18*(6), 1351–1367, doi:10.1890/06-0922.1.

Gholz, H. L. (1982), Environmental limits on above-ground net primary production, leaf-area, and biomass in vegetation zones of the pacific northwest, *Ecology*, *63*(2), 469–481, doi:10.2307/1938964.

Glenn, E. P., A. R. Huete, P. L. Nagler, and S. G. Nelson (2008), Relationship between remotely sensed vegetation indices, canopy attributes and plant physiological processes: What vegetation indices can and cannot tell us about the landscape, *Sensors*, *8*(4), 2136–2160, doi:10.3390/s8042136.

Glenn, E. P., P. L. Nagler, and A. R. Huete (2010), Vegetation index methods for estimating evapotranspiration by remote sensing, *Surv. Geophys.*, *31*(6), 531–555, doi:10.1007/s10712-010-9102-2.

Goldstein, A. H., N. E. Hultman, J. M. Fracheboud, M. R. Bauer, J. A. Panek, M. Xu, Y. Qi, A. B. Guenther, and W. Baugh (2000), Effects of climate variability on the carbon dioxide, water, and sensible heat fluxes above a ponderosa pine plantation in the Sierra Nevada (CA), *Agric. For. Meteorol.*, *101*(2–3), 113–129, doi:10.1016/S0168-1923(99)00168-9.

Goulden, M. (1996), Carbon assimilation and water-use efficiency by neighboring Mediterranean-climate oaks that differ in water access, *Tree Physiol.*, *16*(4), 417–424, doi:10.1093/treephys/16.4.417.

Goulden, M. L., J. W. Munger, S. M. Fan, B. C. Daube, and S. C. Wofsy (1996), Measurements of carbon sequestration by long-term eddy covariance: Methods and a critical evaluation of accuracy, *Global Change Biol.*, *2*(3), 169–182, doi:10.1111/j.1365-2486.1996.tb00070.x.

Goulden, M. L., G. C. Winston, A. M. S. McMillan, M. E. Litvak, E. L. Read, A. V. Rocha, and J. R. Elliot (2006), An eddy covariance mesonet to measure the effect of forest age on land-atmosphere exchange, *Global Change Biol.*, *12*(11), 2146–2162, doi:10.1111/j.1365-2486.2006.01251.x.

Grier, C. C., and S. W. Running (1977), Leaf area of mature northwestern coniferous forests: Relation to site water-balance, *Ecology*, *58*(4), 893–899, doi:10.2307/1936225.

Griffin, J. R. (1973), Xylem sap tension in 3 woodland oaks of central California, *Ecology*, *54*(1), 152–159, doi:10.2307/1934384.

Groeneveld, D. P., W. M. Baugh, J. S. Sanderson, and D. J. Cooper (2007), Annual groundwater evapotranspiration mapped from single satellite scenes, *J. Hydrol.*, *344*(1–2), 146–156, doi:10.1016/j.jhydrol.2007.07.002.

Hellmers, H., J. S. Horton, G. Juhren, and J. O'Keefe (1955), Root systems of some chaparral plants in southern California, *Ecology*, *36*(4), 667–678, doi:10.2307/1931305.

Hubbert, K. R., J. L. Beyers, and R. C. Graham (2001), Roles of weathered bedrock and soil in seasonal water relations of Pinus Jeffreyi and Arctostaphylos patula, *Can. J. For. Res.*, *31*(11), 1947–1957.

Huete, A., K. Didan, T. Miura, E. P. Rodriguez, X. Gao, and L. G. Ferreira (2002), Overview of the radiometric and biophysical performance of the MODIS vegetation indices, *Remote Sens. Environ.*, *83*(1–2), 195–213, doi:10.1016/S0034-4257(02)00096-2.

Hunsaker, C. T., T. W. Whitaker, and R. C. Bales (2012), Snowmelt runoff and water yield along elevation and temperature gradients in California's

southern Sierra Nevada, *J. Am. Water Resour. Assoc.*, *48*, 667–678, doi:10.1111/j.1752-1688.2012.00641.x.

Jeton, A. E., M. D. Dettinger, and J. L. Smith (1996), Potential effects of climate change on streamflow, eastern and western slopes of the Sierra Nevada, *U.S. Geol. Surv. Water Resour. Invest. Rep.*, *95-4260*, 44 pp.

Kings River Conservation District (2003), *The Kings River Handbook*, 4th ed., 41 pp., Fresno, Calif.

Li, Z. L., R. L. Tang, Z. M. Wan, Y. Y. Bi, C. H. Zhou, B. H. Tang, G. J. Yan, and X. Y. Zhang (2009), A review of current methodologies for regional evapotranspiration estimation from remotely sensed data, *Sensors*, *9*(5), 3801–3853, doi:10.3390/s90503801.

Loarie, S. R., P. B. Duffy, H. Hamilton, G. P. Asner, C. B. Field, and D. D. Ackerly (2009), The velocity of climate change, *Nature*, *462*(7276), 1052–1055, doi:10.1038/nature08649.

Lundquist, J. D., and S. P. Loheide II (2011), How evaporative water losses vary between wet and dry water years as a function of elevation in the Sierra Nevada, California, and critical factors for modeling, *Water Resour. Res.*, *47*, W00H09, doi:10.1029/2010WR010050. [Printed *48*(3), 2012.]

Major, J. (1988), California climate in relation to vegetation, in *Terrestrial Vegetation of California*, edited by M. G. Barbour and J. Major, pp. 11–74, Wiley-Interscience, New York.

Moffat, A. M., et al. (2007), Comprehensive comparison of gap-filling techniques for eddy covariance net carbon fluxes, *Agric. For. Meteorol.*, *147*(3–4), 209–232, doi:10.1016/j.agrformet.2007.08.011.

Mu, Q., M. Zhao, and S. W. Running (2011), Improvements to a MODIS global terrestrial evapotranspiration algorithm, *Remote Sens. Environ.*, *115*(8), 1781–1800, doi:10.1016/j.rse.2011.02.019.

Risbey, J. S., and D. Entekhabi (1996), Observed Sacramento Basin streamflow response to precipitation and temperature changes and its relevance to climate impact studies, *J. Hydrol.*, *184*(3–4), 209–223, doi:10.1016/0022-1694(95)02984-2.

Rose, K. L., R. C. Graham, and D. R. Parker (2003), Water source utilization by Pinus jeffreyi and Arctostaphylos patula on thin soils over bedrock, *Oecologia*, *134*(1), 46–54, doi:10.1007/s00442-002-1084-4.

Royce, E. B., and M. G. Barbour (2001a), Mediterranean climate effects. I. Conifer water use across a Sierra Nevada ecotone, *Am. J. Bot.*, *88*(5), 911–918, doi:10.2307/2657044.

Royce, E. B., and M. G. Barbour (2001b), Mediterranean climate effects. II. Conifer growth phenology across a Sierra Nevada ecotone, *Am. J. Bot.*, *88*(5), 919–932, doi:10.2307/2657045.

Ryu, Y., D. D. Baldocchi, S. Ma, and T. Hehn (2008), Interannual variability of evapotranspiration and energy exchange over an annual grassland in California, *J. Geophys. Res.*, *113*, D09104, doi:10.1029/2007JD009263.

Schoenherr, A. A. (1992), *A Natural History of California*, 772 pp., Univ. of Calif. Press, Berkeley, Calif.

Stephenson, N. L. (1998), Actual evapotranspiration and deficit: Biologically meaningful correlates of vegetation distribution across spatial scales, *J. Biogeogr.*, *25*(5), 855–870, doi:10.1046/j.1365-2699.1998.00233.x.

Tague, C., K. Heyn, and L. Christensen (2009), Topographic controls on spatial patterns of conifer transpiration and net primary productivity under climate warming in mountain ecosystems, *Ecohydrology*, *2*(4), 541–554, doi:10.1002/eco.88.

Turnipseed, A. A., P. D. Blanken, D. E. Anderson, and R. K. Monson (2002), Energy budget above a high-elevation subalpine forest in complex topography, *Agric. For. Meteorol.*, *110*(3), 177–201, doi:10.1016/S0168-1923(01)00290-8.

Turnipseed, A. A., D. E. Anderson, P. D. Blanken, W. M. Baugh, and R. K. Monson (2003), Airflows and turbulent flux measurements in mountainous terrain: Part 1. Canopy and local effects, *Agric. For. Meteorol.*, *119*(1–2), 1–21, doi:10.1016/S0168-1923(03)00136-9.

Twine, T. E., W. P. Kustas, J. M. Norman, D. R. Cook, P. R. Houser, T. P. Meyers, J. H. Prueger, P. J. Starks, and M. L. Wesely (2000), Correcting eddy-covariance flux underestimates over a grassland, *Agric. For. Meteorol.*, *103*(3), 279–300, doi:10.1016/S0168-1923(00)00123-4.

Urban, D. L., C. Miller, P. N. Halpin, and N. L. Stephenson (2000), Forest gradient response in Sierran landscapes: The physical template, *Landscape Ecol.*, *15*(7), 603–620, doi:10.1023/A:1008183331604.

U.S. Bureau of Reclamation (2011), Literature synthesis on climate change implications for water and environmental resources, 2nd ed., *Tech. Memo.*, *86-68210-2010-03*, Washington, D. C.

Vicuna, S., and J. A. Dracup (2007), The evolution of climate change impact studies on hydrology and water resources in California, *Clim. Change*, *82*(3–4), 327–350, doi:10.1007/s10584-006-9207-2.

Waring, R. H., and J. F. Franklin (1979), Evergreen coniferous forests of the pacific northwest, *Science*, *204*(4400), 1380–1386, doi:10.1126/science.204.4400.1380.

Whittaker, R. H., and W. A. Niering (1975), Vegetation of Santa Catalina mountains, Arizona. 5. Biomass, production, and diversity along elevation gradient, *Ecology*, *56*(4), 771–790, doi:10.2307/1936291.

Wilson, K., et al. (2002), Energy balance closure at FLUXNET sites, *Agric. For. Meteorol.*, *113*(1–4), 223–243, doi:10.1016/S0168-1923(02)00109-0.

Yuan, W., et al. (2011), Thermal adaptation of net ecosystem exchange, *Biogeosciences*, *8*(6), 1453–1463, doi:10.5194/bg-8-1453-2011.